PROCEEDINGS B

Research

Cite this article: Dolby GA, Hechinger R, Ellingson RA, Findley LT, Lorda J, Jacobs DK. 2016 Sea-level driven glacial-age refugia and post-glacial mixing on subtropical coasts, a palaeohabitat and genetic study. *Proc. R. Soc. B* **283**: 20161571.
http://dx.doi.org/10.1098/rspb.2016.1571

Authors for correspondence:
Greer A. Dolby
e-mail: gadolby@ucla.edu
David K. Jacobs
e-mail: djacobs@ucla.edu

THE ROYAL SOCIETY
PUBLISHING

Sea-level driven glacial-age refugia and post-glacial mixing on subtropical coasts, a palaeohabitat and genetic study

Greer A. Dolby[1], Ryan Hechinger[2], Ryan A. Ellingson[1], Lloyd T. Findley[3], Julio Lorda[4] and David K. Jacobs[1]

[1]Department of Ecology and Evolutionary Biology, University of California, Los Angeles, Los Angeles, CA 90095, USA
[2]Scripps Institution of Oceanography—Marine Biology Research Division, UC San Diego, La Jolla, CA 92093-0218, USA
[3]Centro de Investigación en Alimentación y Desarrollo, A.C.—Unidad Guaymas, Carretera al Varadero Nacional km. 6.6, Colonia Las Playitas, Guaymas, Sonora 85480, México
[4]Facultad de Ciencias, Universidad Autónoma de Baja California. Carretera Transpeninsular Ensenada - Tijuana No. 3917, Colonia Playitas, C.P. 22860, Ensenada, Baja California, México

GAD, 0000-0002-5923-0690

Using a novel combination of palaeohabitat modelling and genetic mixture analyses, we identify and assess a sea-level-driven recolonization process following the Last Glacial Maximum (LGM). Our palaeohabitat modelling reveals dramatic changes in estuarine habitat distribution along the coast of California (USA) and Baja California (Mexico). At the LGM (approx. 20 kya), when sea level was approximately 130 m lower, the palaeo-shoreline was too steep for tidal estuarine habitat formation, eliminating this habitat type from regions where it is currently most abundant, and limiting such estuaries to a northern and a southern refugium separated by 1000 km. We assess the recolonization of estuaries formed during post-LGM sea-level rise through examination of refugium-associated alleles and approximate Bayesian computation in three species of estuarine fishes. Results reveal sourcing of modern populations from both refugia, which admix in the newly formed habitat between the refuges. We infer a dramatic peak in habitat area between 15 and 10 kya with subsequent decline. Overall, this approach revealed a previously undocumented dynamic and integrated relationship between sea-level change, coastal processes and population genetics. These results extend glacial refugial dynamics to unglaciated subtropical coasts and have significant implications for biotic response to predicted sea-level rise.

1. Introduction

Quaternary glacial cycles have shaped genetic variation across the geographical ranges of many taxa by changing global temperatures and the size of glaciers. For instance, cooling and increased ice cover during the Last Glacial Maximum (LGM), about 20 thousand years ago (kya), isolated European populations of boreal species in southerly refugia. Population expansion from these refugia, following glacial retreat, resulted in genetic mixing from multiple sources in newly colonized areas [1–3]. Similarly, ice cover during the LGM also isolated high-latitude coastal marine taxa in ice-free refugia, from which they also mixed following glacial retreat [4,5]. By changing global sea levels, glacial cycles can also connect and isolate populations that occur far from the ice sheets. For example, by exposing the Sunda Shelf, lower LGM-associated sea level permitted the establishment of Asian terrestrial taxa on what were previously and subsequently Indo-Pacific islands (yielding Wallace's Line [6]). Here, we propose that glacially mediated sea-level changes can also strongly influence genetic mixing of marine species far from glaciers. When sea-level change interacts with the variable topography of coastal margins, it can eliminate and
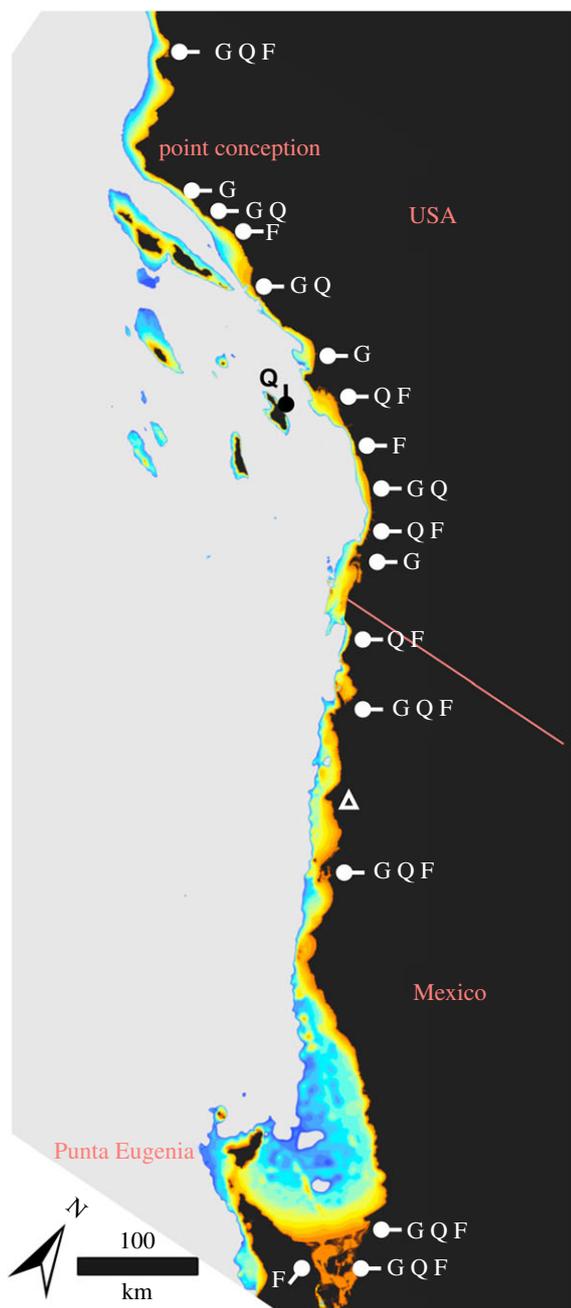
Figure 1. Sample collection and bathymetric map. Bathymetry is contoured at 10 m intervals from 0 to 140 m below present sea level (orange to dark blue, respectively). White markers note sample sites for fish species where: G, *Gillichthys mirabilis*; Q, *Quietula y-cauda*; F, *Fundulus parvipinnis*. Triangle denotes the Cabo Colonet region, which our models predict supported habitat approximately 10 thousand years ago (kya), but does not today. Note the distribution of offshore islands, whose sizes increased with lowered sea level.

reform habitats over time. We examine specifically how this process alters the distribution of habitat through time, affecting the genetic structure of coastal marine populations.

The estuaries of southern Alta and northern Baja California (figure 1) serve as an excellent system to examine how sea-level change can isolate and reconnect populations living in discontinuous coastal habitat. Estuaries in this region are situated along a tectonically steepened and heterogeneous continental shelf [7,8]. Because estuaries only form in certain geomorphic contexts [9], sea-level change would likely have changed the distribution of estuarine habitat over glacial cycles. We, therefore, chose to examine the population genetic structure of three species of co-distributed, low-dispersal estuarine fish

where population history can be inferred on these timescales. These fishes are characteristic of the marine-dominated, large estuaries that we examine here, and are relatively insensitive to salinity variation, simplifying our habitat modelling processes. Further, two of these species were previously studied to ascertain phylogeographic patterns and exhibited separate geographical clades corresponding to southern California and central Baja California [10,11]. Sequence divergences and the absence of modern dispersal barriers led to suggestions of historical isolation through some unspecified mechanism [10,12]. Interpreting these genetic patterns in the context of our prediction of estuarine habitat change over time, we hypothesize that this clade formation was influenced by isolation in estuarine refugia during glacial maxima. In the analysis, we focus on patterns generated during and following the LGM when the shoreline was approximately 130 m lower.

To estimate estuarine palaeohabitat distributions from the LGM to present, we developed and employed habitat modelling with parameters trained on the fishes' modern estuary habitat. To then predict the distribution of historical estuarine habitat, the model used information on historical sea level and modern bathymetry of the continental margin. For our population genetic work, we generated new, highly polymorphic microsatellite and larger mitochondrial DNA (mtDNA) datasets for the two previously studied fishes (*Gillichthys mirabilis*, longjaw mudsucker and *Fundulus parvipinnis*, California killifish) and did the same for the third co-distributed fish (*Quietula y-cauda*, shadow goby). These data permitted analyses of genetic mixing through a novel application of discriminant function analysis (DFA), a commonly used Bayesian clustering algorithm (STRUCTURE) and approximate Bayesian computation (ABC). Based on previously documented genetic patterns [10,11], we predicted that our palaeohabitat models would reveal two primary refugia, one in southern California and one in central Baja California. We also predicted that microsatellite data would: (i) reveal two genetic groupings in accordance with the mitochondrial patterns previously observed, (ii) support a two-refugium scenario with admixture compared to a one-refugium scenario with northern range expansion and (iii) that non-refugium populations would be genetically mixed from populations from both of the inferred refugia (electronic supplementary material, figure S1).

2. Material and methods

(a) Habitat modelling

To predict estuarine palaeohabitat locations, we used two criteria that are essential to tidal estuary formation: shoreline slope and bathymetry [13]. Slope values were parametrized from the 18 modern estuaries in which fish were sampled (electronic supplementary material, table S3). Slopes ranged between 0 and 1.3% (mean = 0.45, median = 0.39). Estuaries were assumed to form at sea level (0 mbpsl $\pm$ 5 m). Importantly, these tidal estuaries are in a rainfall-limited climate where freshwater flow is limited and variable. As a result, these fishes live in a wide range of salinities and temperatures [14–16]. Therefore, we did not include watershed characteristics [17], flow regimes and water chemistries [18] in our models, but these would be important considerations [19] to accurately parametrize a species' niche for estuaries in wetter climates, though these factors may be difficult to hind-cast with certainty (electronic supplementary material).

In ArcGIS (ESRI, Redlands, CA, USA), using a composite sea-level curve [20], we determined slope in a series of 10 m depth
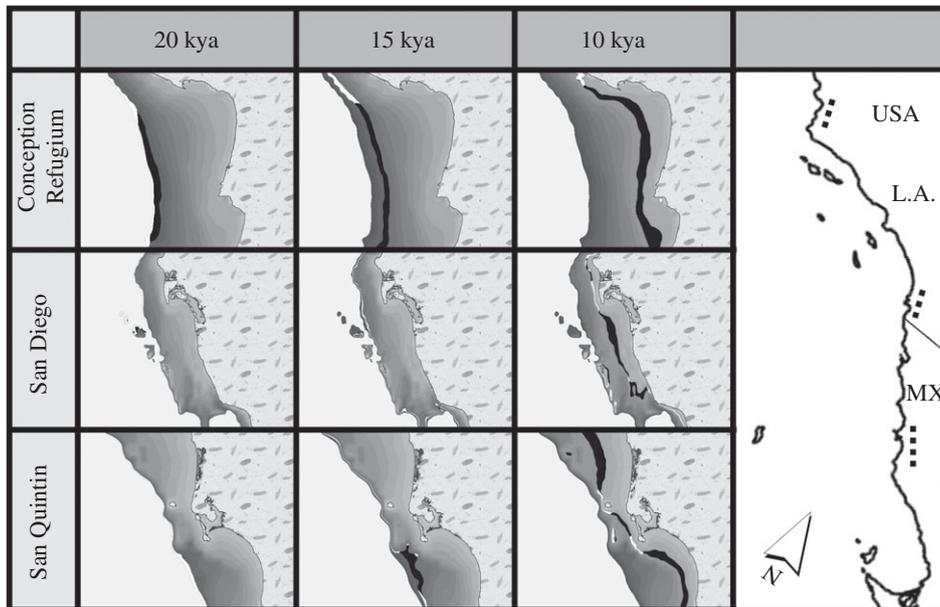
Figure 2. Estuarine habitat distribution through time. Time slices are shown for three latitude-ordered coastal locations (listed left) that correspond to regions dotted on the guide map (right). Area is coloured as inhabitable (black) or too steep to form habitat (white) at 18–20 kya (140–120 mbpsl), approximately 15 kya (110–100 mbpsl), approximately 10 kya (40–30 mbpsl). Bathymetry is contoured in greyscale by 10 m bins; for each map, white on the left represents water and patterned area on the right represents land. Postglacial habitat originates at different times—North Conception (top) is the only refugium among these three locations (see electronic supplementary material, figure S7 for the full coastline time series).

bins covering +5 to 140 m below present sea level (mbpsl) that correspond to sea level from modern (0 kya) to LGM lowstand (20 kya). To locate areas that met the slope criteria (0–1.3%), we queried a 30-arc second digital elevation model [21], which yielded a sequence of depth-specific layers containing polygons of appropriate slope (figures 2 and 3). The coastline was crudely subdivided into regional areas corresponding to modern habitat regions (electronic supplementary material, figure S7). Seven characteristics of these habitat polygons were calculated (e.g. summed polygon area, minimum polygon size) within each depth bin for each coastal region. We note that this parametrization is for tidal estuaries in rainfall-limited climates, not smaller lagoons where the species studied here rarely persist [22,23], nor the classic freshwater-driven estuaries of wetter climates, such as the Atlantic coast of North America.

Previous work [9] classified southern California estuaries qualitatively into types, where physical size was the best differentiating factor. There are specific species assemblages (communities) associated with each estuary type; our fishes are associated with tidal habitat in larger estuaries. We, therefore, used the size attributes of modern habitats where our species occur, and applied these characteristics to the LGM-associated depth bin to identify refugia in which these species would likely occur. To do this we used the modern (0 kya, 0 ± 5 mbpsl) depth bin and species occurrences from this study to determine which polygon attribute(s) best predict modern species occurrences. We first performed a 'habitat' DFA in JMP v11 (SAS Institute Inc., Cary, NC, USA) on the seven polygon attributes separated into two groups. The first group contained modern coastal regions that met slope requirements and where populations of these fishes were present ($N = 6$); the second group contained modern regions that met slope requirements but where populations of these fishes were absent ($N = 2$). Vizcaíno was excluded from this habitat DFA after a robust fit outliers analysis (using Huber and Quartile methods with the default $K = 4$) revealed bias owing to anomalous size. A stepwise variable selection process within the habitat DFA produced two predictive attributes. We entered these predictive attributes into a generalized linear model (GLM) with binomial distribution to determine which coastal region(s) within 130–140 m (20 kya) lowstand depth bin had size attributes that were similar to those of modern estuarine

habitats. The GLMs were calculated with and without Firth's Biased Adjustment estimates to account for small sample sizes and correlated variables. Statistically significant models were run again using a false discovery rate (see the electronic supplementary material, S1).

(b) Genetic mixing

Microsatellite markers were developed via Roche-454 sequencing (electronic supplementary genetic methods, tables S1 and S2). Screening, genotyping and quality control yielded the following number of loci, total number of alleles and sample sizes: *G. mirabilis* (16, 80 and 100), *Q. y-cauda* (17, 148 and 44) and *F. parvipinnis* (20, 199 and 79). To infer population structure, full microsatellite datasets were analysed in STRUCTURE [24] using an admixture model with correlated allele frequencies. Each run included 1 million burnin and 5 million post-burnin replications and was replicated three to five times for *K*s 2–5 for each species. Results were analysed with STRUCTURE HARVESTER [25] and grouped in CLUMPP [26]. Tree reconstruction details for mtDNA and microsatellite data are in the electronic supplementary material, genetic methods.

To explicitly address the relative genetic contribution from inferred refugial sources (Vizcaíno and North Conception populations) to recolonized populations, we regressed the frequency of refugium-associated alleles against coastal distance. Microsatellite genotypic data were converted to allele counts for all individuals per species. We performed DFA without stepwise variable selection using this allele count data with a geographical subset of individuals in two groups: the North Conception Refugium group ($N = 19$, 12 and 26) and the Vizcaíno Refugium group ($N = 14$, 8 and 18) for *G. mirabilis*, *Q. y-cauda* and *F. parvipinnis*, respectively. Alleles determined by DFA to significantly discriminate ($\alpha = 0.05$) between these end-member populations were chosen for subsequent analysis. Each significant allele was designated as 'northern' or 'southern' based on its frequency within these two north and south training groups, and used in the genetic DFA (figure 4*b*). Individuals with missing data for loci with significant alleles were excluded from the analysis, as they would be biased toward lower frequency scores. We summed the frequency
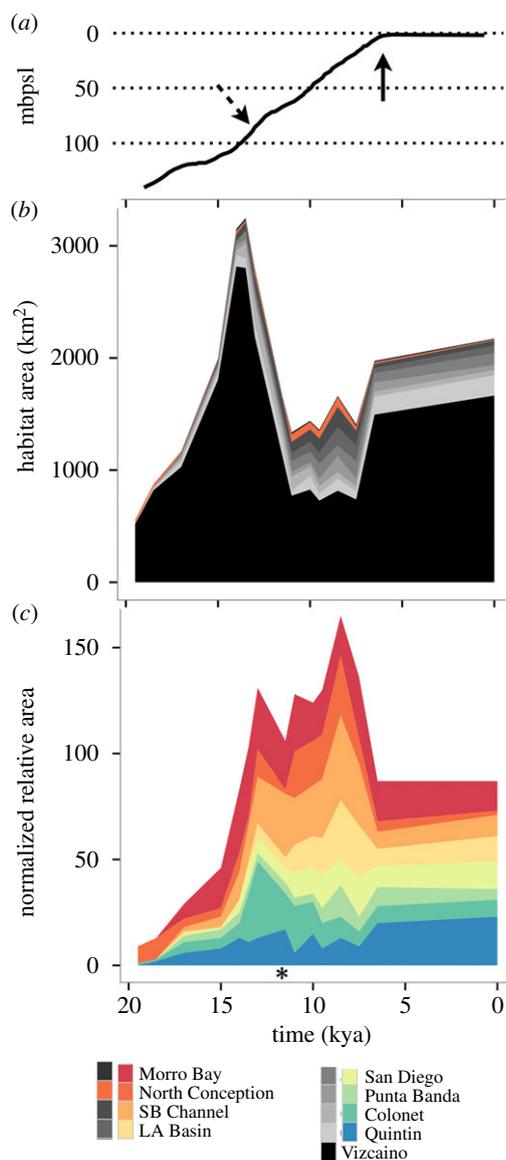
Figure 3. Estuarine habitat abundance through time. (*a*) Sea-level curve adapted from [20]. Dashed arrow indicates meltwater pulse 1A and solid arrow notes onset of modern stillstand. (*b*) Total habitat area quantified through time for nine coastal regions (see electronic supplementary material, figure S8). Vizcaíno refugium is coloured black and drives the overall habitat peak at approximately 14 kya, North Conception refugium is orange, non-refugia are coloured in greyscale (see key). Locations are ordered by latitude. (*c*) Habitat area normalized by coastal area (akin to habitat density) over time. This graph excludes Vizcaíno to show the expansion of southern Californian habitat 15 – 9 kya. Regions are coloured by latitude in a gradient of red (north) to blue (south). Asterisk denotes timing of the Younger Dryas cold period. Time on *x*-axis applies to panels (*a*–*c*).

supplementary material, figure S9). Under scenario 1, the southern and northern populations were modelled as isolated since the LGM and admixed to form the middle group approximately 8 kya. Under scenario 2, the southern population is the only refugium and successively founds the middle and then northern group approximately 8 kya (electronic supplementary material, figure S9, S1, [28]). Posterior values were assessed both directly and logistically per species, and predictive posterior error (PPE) rates were evaluated for each species using all simulations.

3. Results

(a) Habitat modelling

Estimated estuarine habitat area changed dramatically across time and coastal location (figure 3). Total estuarine habitat area (all sites) increased nearly sixfold, from 646 to 3019 km^2, between 20 and 13 kya, before decreasing to 892 km^2 at present (figure 3*b*); mean estuarine habitat area changed from 71 km^2 to 385 km^2 to 241 km^2, respectively. Within southern California, most habitats peaked in size between 12 and 9 kya (figure 3*c*).

The stepwise variable selection process phase of estuarine habitat DFA yielded two variables that classified the presence/absence of our three co-distributed fish taxa with statistical significance. The two significant variables were maximum observed polygon size and total habitat area ($p = 0.01$), which had zero misclassifications when predicting modern distributions for our species. Using these two variables within the lowstand (130–140 mbpsl) palaeohabitat bins, we tested 11 different refugium scenarios. A series of GLMs revealed five statistically supported refugium scenarios. Applying Firth's bias-adjusted corrections and false discovery rate to these five scenarios eliminated four, leaving Vizcaíno + North Conception as the only statistically supported LGM refugium scenario ($p = 0.02$, AICc = 12.9). A Vizcaíno-only, single-refugium scenario was not statistically supported ($p = 0.11$; electronic supplementary material, table S6).

(b) Genetic analyses

STRUCTURE and STRUCTURE HARVESTER analyses of microsatellite data for *G. mirabilis* and *Q. y-cauda* favoured two groups (*K* = 2) using likelihood scores. These groups were a predominantly northern and a southern group, and individuals from populations between the refugia were genetically mixed from the two inferred refugium populations (figure 4*a*). For *F. parvipinnis*, STRUCTURE favoured three groups (northern, central and southern), which could result from allele frequency changes associated with postglacial colonization or an additional factor (see §4).

The genetic DFA used to identify refugium-associated alleles extracted 14, 15 and 39 alleles for *G. mirabilis*, *Q. y-cauda* and *F. parvipinnis*, respectively, that discriminated ($p < 0.05$) between the North Conception refugium and the Vizcaíno refugium.

The results from STRUCTURE and regressions of discriminant alleles for the three species support bidirectional mixing from two sources, consistent with scenario A in electronic supplementary material, figure S1. The northern and southern source (refugium) localities appear genetically distinct and intervening populations appear to be genetic mixtures of those two sources in both analyses (figure 4).

of 'northern' and 'southern' alleles separately for each individual and graphed these sums against geographical coastal distance (figure 4*b*; electronic supplementary material, table S1). Regressions were performed (electronic supplementary material, table S5) to assess how the number of refugium-associated alleles changed with distance between the two purported refugia. All statistical analyses were performed in JMP v11 (SAS Institute Inc.).

Finally, we tested our inferred two-refugium scenario against a possible alternative one-refugium and isolation by distance scenario using DIYABC [27]. We simplified the phylogeographic scenarios by grouping microsatellite data for each species into 'southern,' 'middle' or 'northern' geographical populations and then performed 2 million simulated datasets per species (electronic

Bayesian phylogenetic tree reconstructions using mtDNA for *G. mirabilis* and *Q. y-cauda* reveal both southern and northern clades (electronic supplementary material, figures S2*a* and S3*a*). Intervening populations are mixed as expected under the bidirectional recolonization scenario (electronic supplementary material, figure S1). The mtDNA tree topology for *F. parvipinnis* reveals a northern clade and is otherwise unresolved (electronic supplementary material, figure S4*a*). However, our microsatellite tree recovered northern and southern clades (electronic supplementary material, figure S4*b*), consistent with the previous mtDNA work [10]. Our three microsatellite Neighbour-Joining trees (electronic supplementary material, figures S2*b*, S3*b* and S4*b*) exhibit higher resolution and are generally consistent with the mtDNA trees topologically reflecting two refugial sources.

Relative posterior support from ABC analyses favour a two-refugium model over a one-refugium model for all three species using both direct (0.60, 0.60 and 0.68) and logistic (0.94, 0.70 and 0.94) posterior inferences for *G. mirabilis*, *Q. y-cauda* and *F. parvipinnis*, respectively. These results unambiguously indicate for each of the three species that a Vizcaíno-only refugium scenario with northern range expansion is not supported (see electronic supplementary material). PPE rates for these scenarios were high (0.14–0.23, electronic supplementary material, table S7), but appear to be within the range previously recorded for PPE calculated in DIYABC [29].

4. Discussion

(a) Habitat through time

Our results reveal that coastal steepness reduced tidal estuarine habitat by more than half during the sea-level lowstand (130–140 mbpsl, approx. 20 kya) relative to present day. We find statistical support for two refugia (Vizcaíno refugium and N. Conception refugium, figure 1) separated by approximately 1000 km of uninhabited coast at lowstand (figure 3). We find that, following lowstand, most modern estuarine habitats rapidly formed during the first major meltwater pulse (approx. 15–12 kya, figure 3*a* [20]) and then decreased in size during the present sea-level stasis (approx. 7 kya, figure 3*c*). The inferred 15–12 kya estuarine habitat peak probably occurred as seawater rapidly flooded lower-gradient shelf and valley topography, forming large, open tidal estuaries [30]. Subsequent Holocene estuarine habitat decline is consistent with coastal maturation where wave-generated erosion causes coastal retreat, sediments infill estuaries [31,32], and bar formation at the estuary mouth reduces tidal influence [9]. Such 'bar-built' closed lagoons are smaller, intermittently non-tidal and support different communities from tidal systems studied here [33]. Therefore, the coastal maturation process reduces the abundance of larger systems where the tidal estuarine fishes live [9]. Our detection of end-Pleistocene abundance and Holocene decline of estuarine habitat is supported by previous archaeological and coastal process research that used kitchen-midden deposits and inferred a similar decline of large estuarine habitat over the Holocene [34].

(b) Southern California Bight geomorphic history

The coastal steepness of the Southern California Bight (SCB; defined here as Point Conception to Cabo Colonet, figure 1), which prevented estuary formation during sea-level lowstand, likely resulted from wave protection afforded by the angle of

the SCB [35] and by offshore islands, which emerged in greater number and area during lowstand (figure 1) [36,37]. These features absorb northwesterly wave energy, thus limiting the power of wave attack [38]. Without this buffer, wave action during successive lowstands would have eroded the palaeo-coast [39], forming a lower-slope, more estuary-permissive shelf topography. Supporting this notion, areas more open to wave attack such as N. Conception and Vizcaíno have lower-slope shelf topography and are the sites of lowstand refugia indicated by our habitat models. Ongoing uplift of this region [40] has further reduced the ability of waves to erode the lowstand palaeo-coast by continually exposing lower, steep (uneroded) regions of the shelf. Thus, we propose that regional uplift, the angle of the shoreline and protective offshore topography maintained a steep coastal shelf that limited the formation of tidal estuaries on this section of Pacific coast during glacial lowstand.

(c) Phylogeography

In contrast with refugia invoked *a posteriori* in phylogeography, here our paleohabitat modelling enabled us to form and test hypotheses of northern and southern estuarine refugia suggested by previously observed northern and southern geographical clades [10,11]. Our palaeohabitat models statistically support only a scenario of two refugia (North Conception and Vizcaíno; electronic supplementary material, table S6), which geographically coincide with the previously identified [10,11] southern California and central Baja phyletic clades of *F. parvipinnis* and *G. mirabilis*. We used greater sampling, an additional taxon (*Q. y-cauda*) and new microsatellite data to further evaluate this prediction genetically. Results from ABC using these new genetic data unambiguously favour a two-refugium (Vizcaíno and N. Conception) scenario with admixture of intervening coastline compared with a single-refugium model with northern range expansion (electronic supplementary material, figure S9 table S7). STRUCTURE and genetic DFA analyses show in detail this admixture (figure 4). The replication of this finding for each of three species and its coincidence with the northern (North Conception) and southern (Vizcaíno) refugia, statistically supported by the habitat models, lends robust support to the inference of a two-refugium and postglacial admixture scenario. Given the approximately 0.63 Myr divergence time of the northern and southern mtDNA clades ([41]; see electronic supplementary methods) and their geographical concordance with these refugia, it is likely that similarly located refugia existed during previous lowstands.

While postglacial poleward expansion from a refugium is commonly observed in other taxa (electronic supplementary material, figure S1*b*) [1], here refugium-associated allele frequencies decay bidirectionally with geographical distance (figure 4*b*; electronic supplementary material, figure S1*a*). As predicted, individuals in non-refugium populations appear genetically admixed from the northern and southern refugia in STRUCTURE and geneticDFA results. This bidirectional expansion generated populations that were mixed from genetically distinct sources to produce broadly similar levels of genetic diversity relative to the source refugia (see electronic supplementary material, S1 and figure S5), not a decreased, subsampling of diversity as expected in dispersal from a single source [42]. Potential alternative explanations for unusual allelic patterns such as 'allele surfing' require a
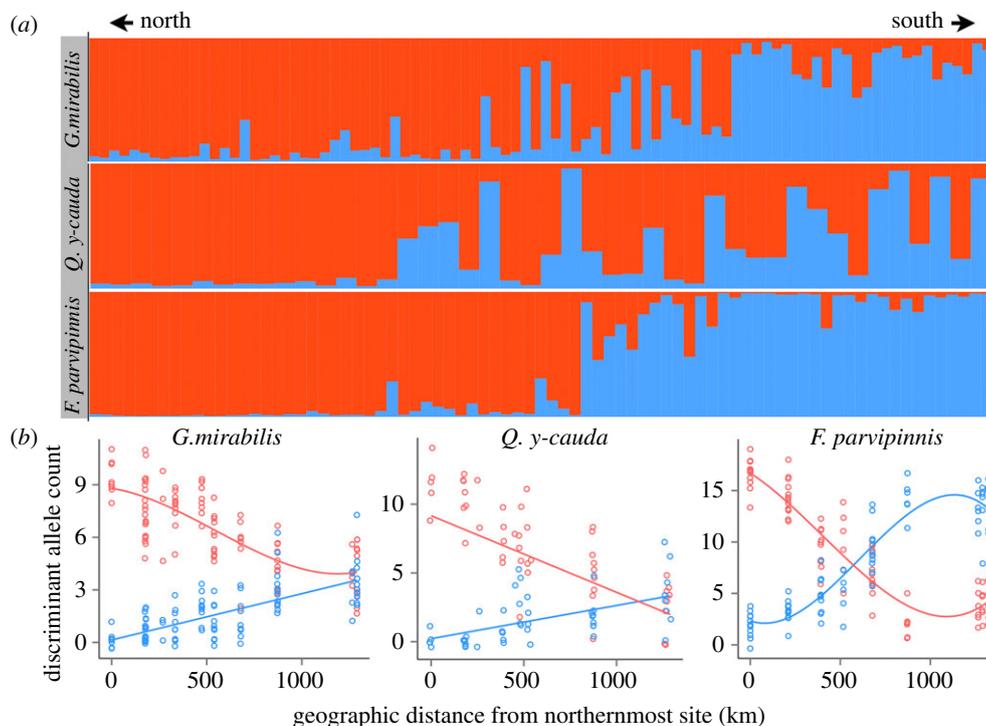
Figure 4. Genetic signatures of refugia and subsequent population mixing. (*a*) Bayesian assignment tests from STRUCTURE using microsatellite data for individuals (vertical bars) ordered north (left, red) to south (right, blue). (*b*) The numbers of northern (red) and southern (blue) discriminant allele counts are shown for all individuals against geographical coastal distance where they were collected. Favoured regressions (AICc) are shown in corresponding colours (see electronic supplementary material, table S5).

continuous expanding front [43], which appears unlikely in taxa with marine dispersal and discontinuous habitat.

While the pattern of bidirectional mixing is observed for all three species, there is also heterogeneity among the species studied. Steepness and shape of the mixing curves differ (figure 4*b*), as does the favoured *K* in STRUCTURE results. These second-order species-specific genetic patterns likely result from ecology and life-history traits that affect dispersal [44]. Interspecific differences in retention within estuaries may apply [10]. For instance, *F. parvipinnis* eggs adhere to estuarine vegetation and their larvae have not been sampled in the near shore plankton [45]. Such limited dispersal could account for the relatively low intrapopulation variance in the DFA discriminant allele scores for *F. parvipinnis* (figure 4*b*). Differential population sizes, fecundities and body sizes may also be factors [46], along with different abilities to persist in bar-built estuaries, which could have occurred undetected by our tidal estuary habitat models. Broadly, the three taxa show less genetic differentiation than small 'bar-built' estuary specialists [47], and more differentiation than species that inhabit both estuaries and open, sandy flats in larger bays [23,48]. Therefore, the size and openness of preferred estuarine habitat may moderate the degree of genetic differentiation of their inhabitants.

In the discriminant allele regressions (figure 4*b*) for *G. mirabilis* and *Q. y-cauda*, the abundance of southern alleles begins to decrease at Bahía San Quintín (BSQ) as expected in the first habitat north of the southern (Vizcaíno) refugium. However, BSQ individuals of *F. parvipinnis* are enriched in southern alleles. A large habitat area is predicted to have arisen early at BSQ (figures 2 and 3*c*). Thus, an early founder event and random drift may have increased the presence of southern alleles in this population [49,50]. Alternatively, low salinity tolerance in this species [14] may have enabled it to persist upstream at BSQ through the LGM. Such upstream habitat would not be reflected in the tidal estuary

habitat models developed here, though in this scenario we would expect BSQ individuals to be more genetically differentiated in STRUCTURE results than we observe (figure 4*a*).

(d) Environmental influences

Many studies have focused on changing temperature during glacial cycles as a control on postglacial expansion ([51], but see [52]). Several factors, however, mitigate the effect of temperature along the southern California coast. The cold California Current, upwelling, and upwelling-induced low clouds and fog along the Pacific coast limit seasonal and latitudinal temperature change relative to, for instance, the Atlantic coast [53], and limit temperature excursions in coastal estuary settings. In addition, in the northern part of our study region, sea-surface temperatures appear to have increased by only 2.7°C between LGM and present [54], which is similar to or less than temperature changes produced by modern El Niño events [55]. Temperature differences in Pacific coast estuaries are also strongly influenced by estuary type and residence time [56]. Thus, in the region of the study, glacial cycle temperature changes are likely to be limited and temperature variability poorly correlated with simple predictors such as latitude or general circulation models. These points and the results of this study indicate that sea-level change and coastal topography are primary drivers of tidal estuary formation in topographically complex, rainfall-limited climates.

5. Conclusion

Our understanding of how glacial–interglacial cycles influenced recent evolution of modern biota is dominated by work on temperate and terrestrial species living on glaciated coastlines, and is often associated with northern range expansion. Such range shifts likely pertain to some coastal regions and

species ([57], but see [58–60]). However, our analysis of south-western North American estuarine fishes reveals that sea-level change and shelf topography interacted to form estuarine refugia separated by long stretches of unoccupied coast during the last glaciation. Postglacial habitat expansion via sea-level rise onto shallower-sloping shelf area was dramatic in the 1000 km-wide inter-refugial coastline. This rapid expansion is associated with genetic mixing between distinct allele sets sourced from distinct refugia, and not expansion to the north of sub-sampled southern alleles (electronic supplementary material, figure S1), as in the case of *F. heteroclitus* on the tectonically passive, lower-grade North American Atlantic coast [61].

These findings were possible through palaeohabitat modelling using physical coastal attributes, comparative molecular work of co-distributed species and an interdisciplinary framework. These techniques should be tested with larger genetic datasets and applied to other habitat types, geographical areas and taxa. Here, they illuminate a previously undocumented process of refugial isolation and recolonization. Similar processes may be important in the evolution of the many coastal species that live in discontinuously distributed habitats. Finally, projected anthropogenic sea-level rise [62] may alter the abundance and distribution of coastal habitat as waters flood new and variable coastal topography. Further modelling is needed to determine the nature of such alterations and the impacts on associated inhabitants.

References

1. Hewitt G. 2000 The genetic legacy of the Quaternary ice ages. *Nature* **405**, 907–913. (doi:10.1038/35016000)

2. Hewitt GM. 2004 Genetic consequences of climatic oscillations in the Quaternary. *Phil. Trans. R. Soc. Lond. B* **359**, 183–195. (doi:10.1098/rstb.2003.1388)

3. Taberlet P, Fumagalli L, Wust-Saucy AG, Cosson JF. 1998 Comparative phylogeography and postglacial colonization routes in Europe. *Mol. Ecol.* **7**, 453–464. (doi:10.1046/j.1365-294x.1998.00289.x)

4. Ilves KL, Huang W, Wares JP, Hickerson MJ. 2010 Colonization and/or mitochondrial selective sweeps across the North Atlantic intertidal assemblage revealed by multi-taxa approximate Bayesian computation. *Mol. Ecol.* **19**, 4505–4519. (doi:10.1111/j.1365-294X.2010.04790.x)

5. Fraser CI, Nikula R, Spencer HG, Waters JM. 2009 Kelp genes reveal effects of subantarctic sea ice during the Last Glacial Maximum. *Proc. Natl Acad. Sci. USA* **106**, 3249–3253. (doi:10.1073/pnas.0810635106)

6. Mayr E. 1944 Wallace's Line in the light of recent zoogeographic studies. *Q. Rev. Biol.* **19**, 1–14. (doi:10.1086/394684)

7. Ingersoll RV, Rumelhart PE. 1999 Three-stage evolution of the Los Angeles basin, southern California. *Geology* **27**, 593–596. (doi:10.1130/0091-7613(1999)027<0593:TSEOTL>2.3.CO;2)

8. Plattner C, Malservisi R, Govers R. 2009 On the plate boundary forces that drive and resist Baja California motion. *Geology* **37**, 359–362. (doi:10.1130/G25360A.1)

9. Jacobs D, Stein ED, Longcore T. 2011 Classification of California estuaries based on natural closure patterns: templates for restoration and management. Southern California Coastal Water Research Project 619, pp. 1–50. (idoi:10.2307/3768203)

10. Bernardi G, Talley D. 2000 Genetic evidence for limited dispersal in the coastal California killifish, *Fundulus parvipinnis*. *J. Exp. Mar. Biol. Ecol.* **255**, 187–199. (doi:10.1016/S0022-0981(00)00298-7)

11. Huang D, Bernardi G. 2001 Disjunct Sea of Cortez–Pacific Ocean *Gillichthys mirabilis* populations and the evolutionary origin of their Sea of Cortez endemic relative, *Gillichthys seta*. *Mar. Biol.* **138**, 421–428. (doi:10.1007/s002270000454)

12. Jacobs DK, Haney TA, Louie KD. 2004 Genes, diversity, and geologic process on the Pacific coast. *Annu. Rev. Earth Planet. Sci.* **32**, 601–652. (doi:10.1146/annurev.earth.32.092203.122436)

13. Kench PS. 1999 Geomorphology of Australian estuaries: review and prospect. *Aust. J. Ecol.* **24**, 367–380. (doi:10.1046/j.1442-9993.1999.00985.x)

14. Griffith RW. 1974 Environment and salinity tolerance in the genus *Fundulus*. *Copeia* **1974**, 319–331. (doi:10.2307/1442526)

15. Feldmeth CR, Waggoner JP. 1972 Field measurements of tolerance to extreme hypersalinity in the California killifish, *Fundulus parvipinnis*. *Copeia* **1972**, 592–594. (doi:10.2307/1442940)

16. Courtois LA. 1976 Respiratory responses of *Gillichthys mirabilis* to changes in temperature, dissolved oxygen and salinity. *Comp. Biochem. Physiol. A Physiol.* **53**, 7–10. (doi:10.1016/S0300-9629(76)80002-3)

17. Dias MS, Oberdorff T, Hugueny B, Leprieur F, Jézéquel C, Cornu J-F, Brosse S, Grenouillet G, Tedesco PA. 2014 Global imprint of historical connectivity on freshwater fish biodiversity. *Ecol. Lett.* **17**, 1130–1140. (doi:10.1111/ele.12319)

18. Whitfield AK, Elliott M, Basset A, Blaber SJM, West RJ. 2012 Paradigms in estuarine ecology—a review of the Remane diagram with a suggested revised model for estuaries. *Estuar. Coast. Shelf Sci.* **97**, 78–90. (doi:10.1016/j.ecss.2011.11.026)

19. Varela S, Lima-Ribeiro MS, Terribile LC. 2015 A short guide to the climatic variables of the Last Glacial Maximum for biogeographers. *PLoS ONE* **10**, e0129037. (doi:10.1371/journal.pone.0129037)

20. Chaytor JD, Goldfinger C, Meiner MA, Huftile GJ, Romsos CG, Legg MR. 2008 Measuring vertical tectonic motion at the intersection of the Santa Cruz-Catalina Ridge and Northern Channel Islands platform, California Continental Borderland, using submerged paleoshorelines. *Geol. Soc. Am. Bull.* **120**, 1053–1071. (doi:10.1130/B26316.1)

21. Becker JJ et al. 2009 Global bathymetry and elevation data at 30 arc seconds resolution: SRTM30_plus. *Mar. Geod.* **32**, 355–371. (doi:10.1080/01490410903297766)

22. Jacobs D, Stein ED, Longcore T. 2010 Classification of California estuaries based on natural closure patterns: templates for restoration and management. Southern California Coastal Water Research Project 619.

8

rspb.royalsocietypublishing.org Proc. R. Soc. B 283: 20161571

23. Earl DA, Louie KD, Bardeleben C, Swift CC, Jacobs DK. 2010 Rangewide microsatellite phylogeography of the endangered tidewater goby, *Eucyclogobius newberryi* (Teleostei: Gobiidae), a genetically subdivided coastal fish with limited marine dispersal. *Conserv. Genet.* **11**, 103–114. (doi:10.1007/s10592-009-0008-9)

24. Pritchard JK, Stephens M, Donnelly P. 2000 Inference of population structure using multilocus genotype data. *Genetics* **155**, 945–959.

25. Earl DA, vonHoldt BM. 2012 STRUCTURE HARVESTER: a website and program for visualizing STRUCTURE output and implementing the Evanno method. *Conserv. Genet. Resour.* **4**, 359–361. (doi:10.1007/s12686-011-9548-7)

26. Jakobsson M, Rosenberg NA. 2007 CLUMPP: a cluster matching and permutation program for dealing with label switching and multimodality in analysis of population structure. *Bioinformatics* **23**, 1801–1806. (doi:10.1093/bioinformatics/btm233)

27. Cornuet J-M, Pudlo P, Veyssier J, Dehne-Garcia A, Gautier M, Leblois R, Marin J-M, Estoup A. 2014 DIYABC v2.0: a software to make approximate Bayesian computation inferences about population history using single nucleotide polymorphism, DNA sequence and microsatellite data. *Bioinformatics* **30**, 1187–1189. (doi:10.1093/bioinformatics/btt763)

28. Dolby GA. 2015 Physical drivers of spatiotemporal genetic patterns and evolutionary processes among and within species of the North American southwest. PhD dissertation, University of California, Los Angeles. See http://escholarship.org/uc/item/90g010gt#.

29. Robert CP, Cornuet J-M, Marin J-M, Pillai NS. 2011 Lack of confidence in approximate Bayesian computation model choice. *Proc. Natl Acad. Sci. USA* **108**, 15 112–15 117. (doi:10.1073/pnas.1102900108)

30. Upson JE. 1949 Late Pleistocene and Recent changes of sea level along the coast of Santa Barbara County, California. *Am. J. Sci.* **247**, 94–115. (doi:10.2475/ajs.247.2.94)

31. Sommerfield CK, Lee HJ. 2004 Across-shelf sediment transport since the Last Glacial Maximum, southern California margin. *Geology* **32**, 345–348. (doi:10.1130/G20182.2)

32. Knott JR, Eley DS. 2006 Early to Middle Holocene coastal dune and estuarine deposition, Santa Maria Valley, California. *Phys. Geogr.* **27**, 127–136. (doi:10.2747/0272-3646.27.2.127)

33. Swift CC, Haglund TR, Ruiz M, Fisher RN. 1993 The status and distribution of the freshwater fishes of southern California. *Bull. South. Calif. Acad. Sci.* **92**, 101–167.

34. Masters PM. 2006 Holocene sand beaches of southern California: ENSO forcing and coastal processes on millennial scales. *Palaeogeogr. Palaeoclimatol. Palaeoecol.* **232**, 73–95. (doi:10.1016/j.palaeo.2005.08.010)

35. Sunamura T. 1976 Feedback relationship in wave erosion of laboratory rocky coast. *J. Geol.* **84**, 427–437. (doi:10.2307/30066060)

36. Graham MH, Dayton PK, Erlandson JM. 2003 Ice ages and ecological transitions on temperate coasts. *Trends Ecol. Evol.* **18**, 33–40. (doi:10.1016/S0169-5347(02)00006-X)

37. Kinlan BP, Graham MH. 2005 Late-Quaternary changes in the size and shape of the California Channel Islands: implications for marine subsidies to terrestrial communities. In *Proc. of the California Islands Symp.*, Vol. 6, pp. 131–142 (eds DK Garcelon, CA Schwemm). Arcata, CA: Institute for Wildlife Studies.

38. Kirby JT, Dalrymple RA. 1986 Modeling waves in surfzones and around islands. *J. Waterw. Port Coast. Ocean Eng.* **112**, 78–93. (doi:10.1061/(ASCE)0733-950X(1986)112:1(78))

39. Benumof BT, Storlazzi CD, Seymour RJ, Griggs GB. 2000 The relationship between incident wave energy and seacliff erosion rates: San Diego County, California. *J. Coast. Res.* **16**, 1162–1178. (doi:10.2307/4300134)

40. Niemi NA, Oskin M, Rockwell TK. 2008 Southern California earthquake center geologic vertical motion database. *Geochem. Geophys. Geosyst.* **9**, 1–14. (doi:10.1029/2008GC002017)

41. Ellingson RA, Swift CC, Findley LT, Jacobs DK. 2014 Convergent evolution of ecomorphological adaptations in geographically isolated Bay gobies (Teleostei: Gobionellidae) of the temperate North Pacific. *Mol. Phylogenet. Evol.* **70**, 464–477. (doi:10.1016/j.ympev.2013.10.009)

42. Petit RJ. 2003 Glacial refugia: hotspots but not melting pots of genetic diversity. *Science* **300**, 1563–1565. (doi:10.1126/science.1083264)

43. Excoffier L, Ray N. 2008 Surfing during population expansions promotes genetic revolutions and structuration. *Trends Ecol. Evol.* **23**, 347–351. (doi:10.1016/j.tree.2008.04.004)

44. Bilton DT, Paula J, Bishop JD, D. 2002 Dispersal, genetic differentiation and speciation in estuarine organisms. *Estuar. Coast. Shelf Sci.* **55**, 937–952. (doi:10.1006/ecss.2002.1037)

45. Watson W. 1996 *The early stages of fishes in the California current region*. California Cooperative Oceanic Fisheries Investigations, Atlas No. 33. Lawrence, KS: Allen Press.

46. Waples RS. 1991 Heterozygosity and life-history variation in bony fishes: an alternative view. *Evolution* **45**, 1275–1280. (doi:10.2307/2409733)

47. Dawson MN, Staton JL, Jacobs DK. 2001 Phylogeography of the tidewater goby, *Eucyclogobius newberryi* (Teleostei, Gobiidae), in coastal California. *Evolution* **55**, 1167–1179. (doi:10.1111/j.0014-3820.2001.tb00636.x)

48. Dawson MN, Louie KD, Barlow M, Jacobs DK, Swift CC. 2002 Comparative phylogeography of sympatric sister species, *Clevelandia ios* and *Eucyclogobius newberryi* (Teleostei, Gobiidae), across the California Transition Zone. *Mol. Ecol.* **11**, 1065–1075. (doi:10.1046/j.1365-294X.2002.01503.x)

49. Allendorf FW. 1986 Genetic drift and the loss of alleles versus heterozygosity. *Zoo Biol.* **5**, 181–190. (doi:10.1002/zoo.1430050212)

50. Pardo LM, MacKay I, Oostra B, van Duijn CM, Aulchenko YS. 2005 The effect of genetic drift in a young genetically isolated population. *Ann. Hum. Genet.* **69**, 288–295. (doi:10.1046/j.1529-8817.2005.00162.x)

51. Waltari E, Hickerson MJ. 2013 Late Pleistocene species distribution modelling of North Atlantic intertidal invertebrates. *J. Biogeogr.* **40**, 249–260. (doi:10.1111/j.1365-2699.2012.02782.x)

52. Gaylord B, Gaines SD. 2000 Temperature or transport? Range limits in marine species mediated solely by flow. *Am. Nat.* **155**, 769–789. (doi:10.1086/303357)

53. Yamamoto M. 2009 Response of mid-latitude North Pacific surface temperatures to orbital forcing and linkage to the East Asian summer monsoon and tropical ocean–atmosphere interactions. *J. Quat. Sci.* **24**, 836–847. (doi:10.1002/jqs.1255)

54. Lyle M, Heusser L, Ravelo C, Andreasen D, Olivarez Lyle A, Diffenbaugh N. 2010 Pleistocene water cycle and eastern boundary current processes along the California continental margin. *Paleoceanography* **25**, PA4211–19. (doi:10.1029/2009PA001836)

55. Thunell R, Tappa E, Pride C, Kincaid E. 1999 Sea-surface temperature anomalies associated with the 1997–1998 El Niño recorded in the oxygen isotope composition of planktonic foraminifera. *Geology* **27**, 843–846. (doi:10.1130/0091-7613(1999)027<0843:SSTAAW>2.3.CO;2)

56. Spies BT, Steele MA. 2016 Effects of temperature and latitude on larval traits of two estuarine fishes in differing estuary types. *Mar. Ecol. Prog. Ser.* **544**, 243–255. (doi:10.3354/meps11552)

57. Edmands S. 2001 Phylogeography of the intertidal copepod *Tigriopus californicus* reveals substantially reduced population differentiation at northern latitudes. *Mol. Ecol.* **10**, 1743–1750. (doi:10.1046/j.0962-1083.2001.01306.x)

58. Dawson MN. 2001 Phylogeography in coastal marine animals: a solution from California? *J. Biogeogr.* **28**, 723–736. (doi:10.1046/j.1365-2699.2001.00572.x)

59. Kelly RP, Palumbi SR. 2010 Genetic structure among 50 species of the northeastern Pacific rocky intertidal community. *PLoS ONE* **5**, e8594. (doi:10.1371/journal.pone.0008594)

60. Marko PB. 2004 'What's larvae got to do with it?' Disparate patterns of post-glacial population structure in two benthic marine gastropods with identical dispersal potential. *Mol. Ecol.* **13**, 597–611. (doi:10.1046/j.1365-294X.2004.02096.x)

61. Adams SM, Lindmeier JB, Duvernell DD. 2006 Microsatellite analysis of the phylogeography, Pleistocene history and secondary contact hypotheses for the killifish, *Fundulus heteroclitus*. *Mol. Ecol.* **15**, 1109–1123. (doi:10.1111/j.1365-294X.2006.02859.x)

62. Church JA et al. 2013 Sea level change. In *Climate Change 2013: the physical science basis. contribution of working group I to the fifth assessment report of the Intergovernmental Panel on Climate Change* (eds TF Stocker et al.), pp. 1137–1216. Cambridge, UK and New York, NY: Cambridge University Press.

63. Dolby GA, Hechinger R, Ellingson RA, Findley LT, Lorda J, Jacobs DK. 2016 Data from: Sea-level driven glacial-age refugia and post-glacial mixing on subtropical coasts, a palaeohabitat and genetic study. Dryad Digital Repository. (http://dx.doi.org/10.5061/dryad.46092)